Materials Research, Vol. 6, No. 4, 563-568, 2003.

Influence of Ni Content on Physico-Chemical Characteristics of Ni, Mg, Al-Hydrotalcite Like Compounds

Alexandre Carlos Camacho Rodrigues[a]*, *Cristiane Assumpção Henriques*[b], *José Luiz Fontes Monteiro*[a]

[a]*Núcleo de Catálise (NUCAT) -COPPE/UFRJ*
C.P. 68502, 21945-970 Rio de Janeiro - RJ, Brazil
[b]*Instituto de Química/UERJ, Rua São Francisco Xavier, 524*
20559-900 Rio de Janeiro - RJ, Brasil

Received: October 30, 2002; Revised: August 24, 2003

The physico-chemical properties of a series of Ni,Mg,Al-HTLC with Al/(Al+Mg+Ni) = 0.25 and low Ni/Mg ratios were studied by means of X-ray diffraction (XRD), thermogravimetric (TGA) and thermodifferential (DTA) analysis, N_2 physisorption and temperature programmed reduction (TPR). The as-synthesized materials were well-crystallized, with XRD patterns typical of the HTLCs in carbonate form. Upon calcination and dehydration the dehydroxilation of the layers with concurrent decomposition of carbonate anions produced mixed oxides with high surface area. XRD analysis indicated that the different nickel and aluminum oxides species are well-dispersed in a poor-crystallized MgO periclase-type phase. As observed by TPR, the different Ni species showed distinct interactions with Mg(Al)O phase, which were influenced by both nickel content and calcination temperature. Regardless of the the nickel content, the reduction of nickel species was not complete as indicated by the presence of metallic dispersions.

Keywords: *hydrotalcites, nickel, mixed oxides, Ni,Mg,Al-HTLC*

1. Introduction

Hydrotalcite like compounds (HTLCs) are layered-double hydroxides (LDHs) with lamellar structure and general formula $(M^{2+}_{1-x}M^{3+}_{x}(OH)_2)^{x+}(A^{m-}_{x/m}).nH_2O$ (where M^{2+} = Mg^{2+}, Zn^{2+}, Ni^{2+}, Co^{2+}; M^{3+} = Al^{3+}, Fe^{3+}, Cr^{3+} and A = OH^-, Cl^-, NO_3^-, CO_3^{2-}), x taking values between 0.20 and 0.33[1]. These materials have similar structure to that of brucite ($Mg(OH)_2$), where each Mg^{2+} ions is octahedrally surrounded by six OH^- ions and the different octahedra share edges to form infinite sheets[1-4]. The sheets are stacked one on top of the other and are held together by weak interactions through hydrogen bonds[1-3]. When M^{2+} cations are replaced isomorphously by M^{3+} ones with similar radius, the brucite-like layers become positively charged and the electrical neutrality is attained by compensating anions located in the interlayers along with water molecules[1,2].

They can be easily synthesized using different methods[1], the most common being the co-precipitation at constant pH of diluted solutions containing M^{2+} and M^{3+} cations with solutions containing carbonate and hydroxide ions[4-6]. The precipitate is quite amorphous, but after ageing by hydrothermal or thermal treatments the crystallinity is improved[7].

HTLCs have many industrial applications, particularly in the calcined form. The calcination of HTLCs induces dehydration, dehydroxilation and loss of compensation anions, forming the mixed oxides with basic properties and a poorly crystallized structure[3,4,7,8]. These oxides show small particle size, large specific surface area, homogeneous interdispersion of the metals and a better resistance to sintering than the corresponding supported catalysts. The surface basic properties and/or redox properties depends on their chemical composition, preparation methods and treatment conditions[6,9-13]. Due to the wide variety of chemical compositions, they are very efficient catalysts in different reactions. Mg,Al-mixed oxides, for example, are active for base-catalyzed reactions such as aldol condensation of aldehydes and ketones, condensation of the carbonyl group

*e-mail: camacho@peq.coppe.ufrj.br
Trabalho apresentado no V Encontro da Sociedade Brasileira de Crescimento de Cristais, Guarujá - SP, 2002.

with compounds presenting methylene activated groups (for example, Knoevenagel and Claisen-Schmidt reactions), alkene isomerization, alkylation of diketones and phenols, alkene epoxidation activated by hydrogen peroxide[4,10-12,14-21]. HTLCs containing transition metals such as Ni, Co, Cu or Zn or noble metals such as Rh and Ru[22-27] have also been used as precursors for hydrogenation or redox catalysts for methanol synthesis from syngas[28], removal of SOx and NOx from FCC effluents[29,30] and other redox reactions.

Ni,Mg,Al-mixed oxides derived from HTLCs are among the most studied systems due to their good catalytic performance on partial oxidation of methane[31], hydrogenation of nitriles into primary amines[32,33] and, more recently, on MIBK (methyl-isobutyl-ketone) one step synthesis from acetone and H_2[34,35]. Their basic properties are strongly dependent on the calcination temperature of the precursor while the reducibility of the Ni phase decreased when either the Mg content or the calcination temperature increased[36,37].

Although there are some papers in the literature concerning the properties of Ni,Mg,Al-mixed oxides with high Ni/Mg ratios[32,33,36,37], little is known about similar systems with low Ni contents. Our particular interest in these systems is associated to their potential use as catalyst for MIBK synthesis[35]. So, in the present work we investigated the influence of nickel content on physico-chemical characteristics (such as thermal stability, texture and reducibility) of Ni,Mg,Al-HTLCs. These materials will be further used as precursors of the Ni,Mg,Al-mixed oxides that will catalyze the one-step synthesis of methyl-isobutyl-ketone (MIBK) from acetone and hydrogen (H_2) at atmospheric pressure. High acetone conversion and MIBK selectivity, under these conditions, is a matter of interest due to the drawbacks of the current commercial process.

2. Materials and Methods

2.1. Ni,Mg,Al-HTLC synthesis

Hydrotalcite samples were prepared by coprecipitating at room temperature an aqueous solution of nickel, magnesium and aluminum cations (solution A) with a highly basic carbonate solution (solution B). Solution A, containing $Ni(NO_3)_2.6H_2O$, $Mg(NO_3)_2.6H_2O$ and $Al(NO_3)_3.9H_2O$ dissolved in distilled water was 1.5 M in (Al+Mg+Ni) with an Al/(Al+Mg) molar ratio equal to 0.25 and a Ni/Mg molar ratio of 1/5, 1/15, 1/25, 1/50 or 1/100. Solution B was prepared dissolving appropriated amounts of Na_2CO_3 and NaOH in distilled water in order to obtain a $[CO_3^{2-}]$ equal to 1.0 M and a pH equal to 13 during the aging of the gel. In the synthesis procedure, solution A was slowly dropped (60 ml/h) under vigorous stirring to a B solution placed in a 150 ml PTFE reactor. The gel formed was aged under constant pH (13) for 18 h at 333 K. The solid obtained was then filtered and washed with distilled water (363 K) until pH 7. The Ni,Mg,Al-hydrotalcites so obtained were then dried at 353 K overnight. They were named NiHTXX, where *XX* is related to the Mg/Ni molar ratio.

The Ni,Mg,Al-mixed oxides were produced by calcination of HTLCs under dry air, using a heating rate of 10 K/min, from room temperature to the desired one (723 or 1023 K) and keeping at this temperature for 2 h (1023 K) or 10 h (723 K). The calcined samples were named CNiHTXX(T), where T is the calcination temperature.

2.2. Physico-chemical characterization

The chemical composition of the synthesized samples was determined by X-ray fluorescence using a Rigaku spectrometer. X-ray powder diffraction patterns were recorded in a Rigaku X-ray generator diffractometer with a graphite monochromator using Cu Kα radiation and varying 2θ values from 5 to 80°. Accurate unit cell parameters were determined by cell refinement using UnitCell software[38]. Thermal decomposition of the HTLCs samples was evaluated by TGA and DTA analyses carried out in a Rigaku Thermobalance TAS 100. Around 10.00 mg of the material was heated to 1273 K at 10 K/min under dry air flow.

The textural characteristics, such as BET specific area, external area (t-plot method) and pore volume (BJH method), were determined by N_2 adsorption-desorption at 77 K in a Micromeritics ASAP 2000. Prior to the analyses the samples were outgassed for 20 h at 473 K.

The calcined samples were analyzed by temperature programmed reduction (TPR), carried out in a microflow reactor operating at atmospheric pressure, under H_2 atmosphere (0.53% H_2/Ar) in the range of 298 to 1123 K, using a heating rate of 5 K/min and keeping at 1123 K for 2 h. The outflowing gases were accompanied by on-line mass spectrometry using a Balzers quadrupole spectrometer (model PRISMA-QMS 200). The release of hydrogen (m/z = 2), water (m/z = 18) and carbon dioxide (m/z = 12, 28 and 44) was monitored.

3. Results and Discussion

The chemical composition of the synthesized samples is presented in Table 1. They are similar to those of the gel of synthesis, indicating an approximately complete incorporation of the cations in HTLC structure.

The XRD patterns of the Ni,Mg,Al-HTLC samples are shown in Fig. 1. They exhibit sharp and symmetrical reflections for (003), (006), (110) and (113) planes and broad and asymmetric reflections for (102), (105) and (108) planes, characteristic of a well-crystallized HTLC in carbonate form. No other phase was detected, suggesting that both Ni^{2+} and Al^{3+} have isomorphically replaced Mg^{2+} cations in the brucite-like layers.

Table 1. Chemical composition and structural characteristics of the as-synthesized samples.

Sample	Al/(Al+Mg+Ni)	Mg/Ni	*a* (Å)	*c* (Å)	S_{BET} (m^2/g)	V_{meso} [a] (cm^3/g)
NiHT5	0.24	5.4	3.05	23.11	82.2	0.493
NiHT15	0.24	15.1	3.06	23.32	78.3	0.488
NiHT25	0.24	24.7	3.06	23.20	62.3	0.426
NiHT50	0.24	50.1	3.06	23.17	68.7	0.366
NiHT100	0.24	106.8	3.06	23.31	74.9	0.533

[a]BJH method, adsorption branch (20-1000Å)

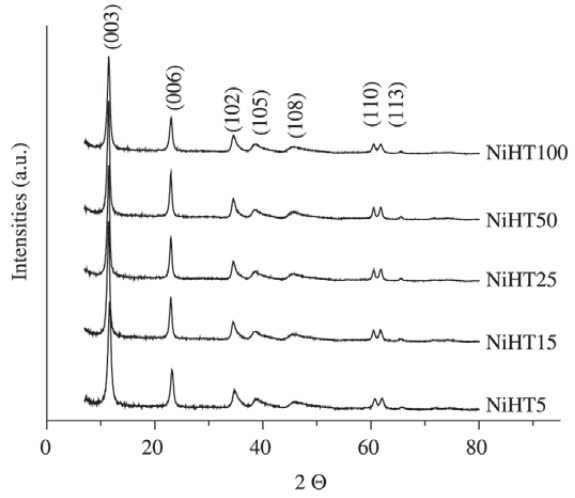

Figure 1. X-ray diffractograms for the as-synthesized Ni, Mg, Al-HTLC samples.

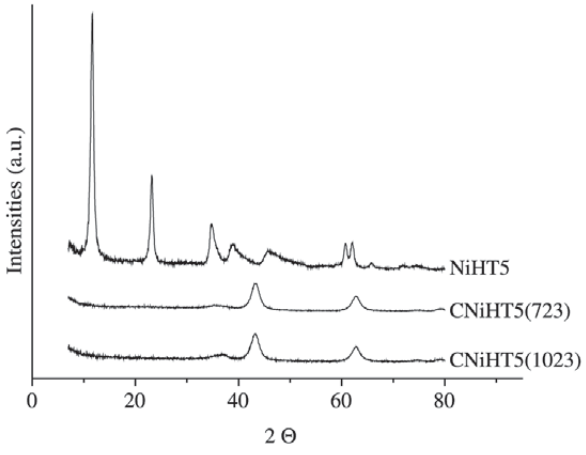

Figure 2. X-ray diffractograms for NiHT5 as-synthesized and calcined at 723 K (CNiHT5(723)) and 1023 K (CNiHT5(1023)).

For the classical rhombohedral 3R stacking symmetry of hydrotalcites, the lattice parameters are ***a*** (associated to the cation-cation distance in the hydroxide layer) and ***c=3c'*** (where c' is the thickness of one layer of the brucite-like sheet and one interlayer)[1]. The lattice parameters for the synthesized samples, determined from the positions of the lines corresponding to crystallographic planes (003), (006), (110) and (113), are shown in Table 1. It can be observed that they are in agreement with those reported on literature for this type of material[33,37].

For all samples, after calcination up to 723 or 1023 K, the characteristic lamellar structure disappears and XRD patterns show the presence of poor crystallized MgO periclase-type phase (peaks at 2θ equal to 35.70°, 43.40° and 62.90°), as illustrated in Fig. 2 for sample NiHT5. These results indicate that both nickel and aluminum oxides are well dispersed in MgO matrix, without the segregation of a spinel-phase. There are some divergences in the literature with respect to the calcination temperature of HTLCs that lead to the formation of the spinel[1,5,8,36,37]. However, our results seem to agree with those that propose temperatures above 1073 K.

Figure 3 shows the TGA and DTA profiles for the synthesized HTLCs. The results indicate two endothermic losses of weight characteristic of the HTLCs in carbonate form [1,2,5-8,13,33,37]. The first loss, with the minimum at about 481-486 K, can be attributed to the loss of interlayer water, whereas the second one, with the minimum in the range of 653 to 663 K, is due to elimination of the carbonate ions from the interlayer and the hydroxide ions from the brucite-like layers.

The thermal decomposition of the studied samples is not influenced by its Ni/Mg ratio, since both temperature maxima and weight losses (18-20 wt.%, for the first loss, and 23-24.5 wt.%, for the second) determined by TGA/DTA were quite similar for all samples. These values are close to those reported for pure hydrotalcites in accordance with the relatively low Ni content on the studied samples.

Textural characteristics of the as-synthesized samples were also not significantly influenced by differences in Ni content, as shown in Table 1. Specific surface areas are relatively low (60 to 80 m^2/g), which is consistent with the IUPAC-type II N_2 adsorption isotherms observed for the samples. These curves are typical of non-porous/macroporous solids or mesoporous solids having slit-shaped pores among parallel layers. The IUPAC-type H1 hysteresis loop observed in the isotherms for $p/p_0 > 0.8$ associated with the broad pore diameters distribution (100 to 800 Å) presented by the samples may indicate that part of the pore volume (Table 2) should correspond to the filling of the interparticle space[39].

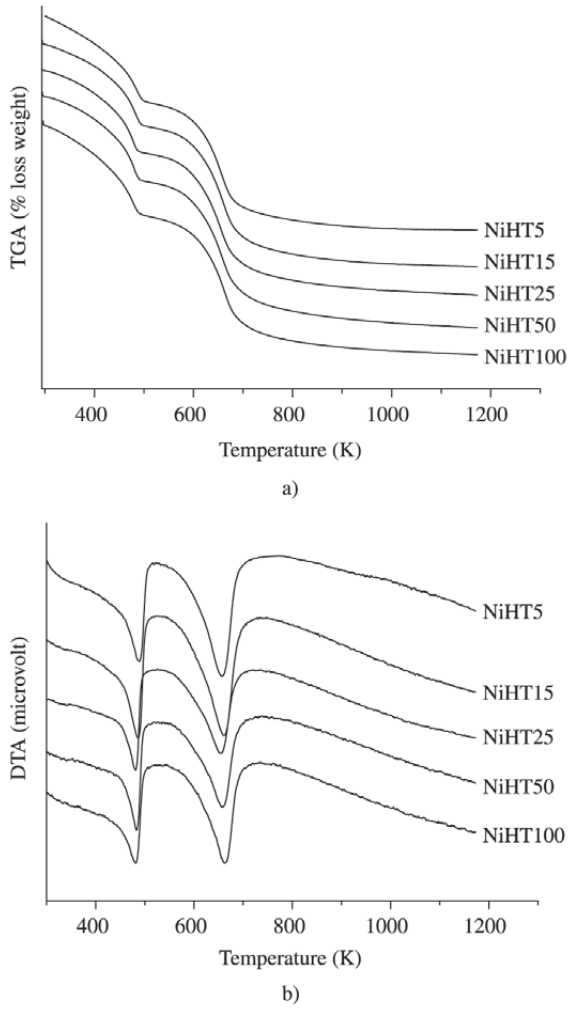

Figure 3. a) TGA curves; b) DTA profiles of the Ni, Mg, Al-HTLC samples.

Table 2. Textural characteristics of HT5 as-synthesized and calcined at different temperatures.

Sample	S_{BET} (m^2/g)	V_{meso} [a] (cm^3/g)
NiHT5	82.2	0.493
CNiHT5(723)	254.2	0.712
CNiHT5(1023)	223.3	0.667

[a]BJH method, adsorption branch (20-1000Å)

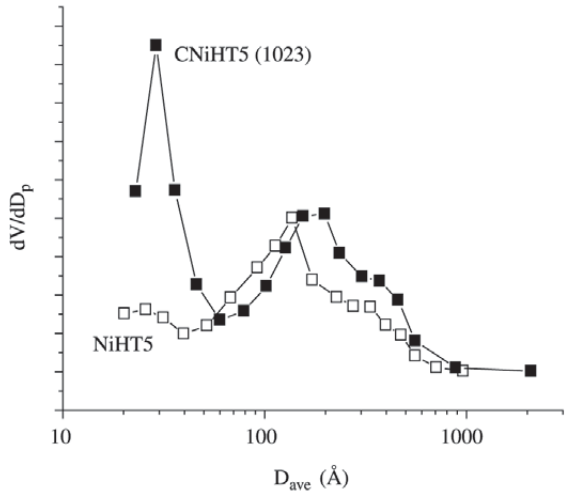

Figure 4. Pore size distribution for NiHT5 and CNiHT5 (1023 K) samples.

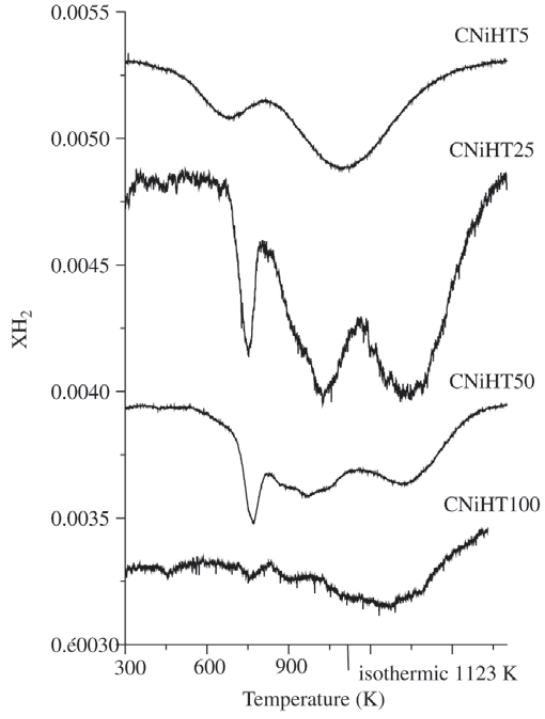

Figure 5. Thermoprogrammed reduction profile of calcined samples (723 K).

Upon calcination both specific surface areas and pore volumes increase, mainly due the formation of mesopores with diameter in the range of 20 to 50 Å, as shown in Table 2 and Fig. 4 for sample NiHT5. The formation of this mesopores can be associated to the elimination of carbonate anions, as CO_2, beginning at about 550 K and leading to partial destruction of the layered structure (as observed by XRD) giving rise to holes, the so-called "craters"[8]. This "cratering" of the samples could be responsible for the observed increase in surface area and pore volume.

The TPR profiles of the Ni,Mg,Al-HTLC samples after calcination at 723K are given in Fig. 5. Except for the sam-

ple with the highest Ni content (CNiHT5), three peaks of hydrogen consumption are observed, corresponding to three different reducible species.

The first hydrogen consumption, with a maximum ranging from 740 to 770 K, can be assigned to the reduction of nickel oxide weakly interacted with the Mg(Al)O phase (Eq. 1). The increase in the Ni content promoted a weakening of this interaction, resulting in lower reduction temperatures. The decrease in NiO reducibility with the decrease in Ni content was also reported on literature[36] and may be attributed to the increase on the effect of the presence of foreign ions (Mg^{2+} and/or mainly Al^{3+}) inside the NiO phase.

$$NiO + H_2 \leftrightarrow Ni^0 + H_2O \quad (1)$$

The temperature range for reduction of NiO in Ni,Mg,Al mixed oxides is higher than that reported for the reduction of supported NiO[34], confirming that the homogeneous interdispersion of the elements in HTLCs gives rise to a strong interaction among them in the correspondent mixed oxide.

The second peak, with maxima between 890 and 1023 K, can be associated to the reduction of non stoichiometric amorphous nickel aluminate or nickel oxide strongly interacted with the Mg(Al)O phase[40] (Eq. 2).

$$Ni_xAl_2O_{3+x} + x\ H_2 \leftrightarrow x\ Ni^0 + x\ H_2O + Al_2O_3 \quad (2)$$

The third peak was observed on the isothermic step at 1123 K. The reduction of stoichiometric $NiAl_2O_4$ species (Eq. 3) can be pointed as responsible for this hydrogen consumption at high temperature.

$$NiAl_2O_4 + H_2 \leftrightarrow Ni^0 + H_2O + Al_2O_3 \quad (3)$$

Since this spinel phase was not detected by XRD for calcined samples (Fig. 2), its formation could occur due to the heating of the sample at temperatures higher than 1073 K, during TPR analysis.

The consumption of hydrogen for the sample CNiHT5, CNiHT25 and CNiHT50, calcined at 723 K, was determined from the areas under the curves presented in Fig. 5. The TPR profile for sample NiHT100 was not clearly accompanied due to both the low sensitivity of hydrogen on mass spectrometry and the low Ni content of this sample. The results indicate that although the Ni content influences the reduction profiles of the different Ni species it has no significant effect on H_2 consumption, since the values of metallic dispersion are similar for the three samples evaluated (65% to 80%).

These results indicates an incomplete reduction of the nickel species present and confirms the lower reducibility of nickel on the Ni,Mg,Al mixed oxides with low Ni content, when compared to that observed for Ni-rich similar materials[37].

Figure 6 compares the H_2 consumption profiles of sample NiHT5 calcined at 723 K (CNiHT5(723)) and at 1023 K (CNiHT5(1023)). They are quite different, indicating that the calcination temperature influences both the type of nickel-oxides species formed upon the thermal treatment under air and their interaction with the Mg(Al)O phase. The increase in the temperature of calcination decreases the reducibility of Ni species (low H_2 consumption). As proposed by Fornasari *et al.*[36], the lower reducibility observed for the sample calcined up to 1023 K may be explained by a lower accessibility of the sample to the reducing gas, probably due to the presence of a non-stoichiometric spinel type phase, not detected by XRD, decorating the NiO particles.

Conclusions

Well-crystallized Ni, Mg, Al-HTLC with Ni/Mg ratios in the range between 1/5 and 1/100 were synthesized. Their thermal stability, evaluated by TGA/DTA, indicated two defined weight losses, the first, corresponding to the loss of interlayer water, and the second, associated to dehydroxilation and decarbonatation. For the Ni/Mg ratios studied, the nickel content does not influenced thermal stability of the HTLCs. Upon calcination, the lamellar structure of HTLC disappeared and the formation of a poor crystallized MgO-periclase phase was observed. No other phases

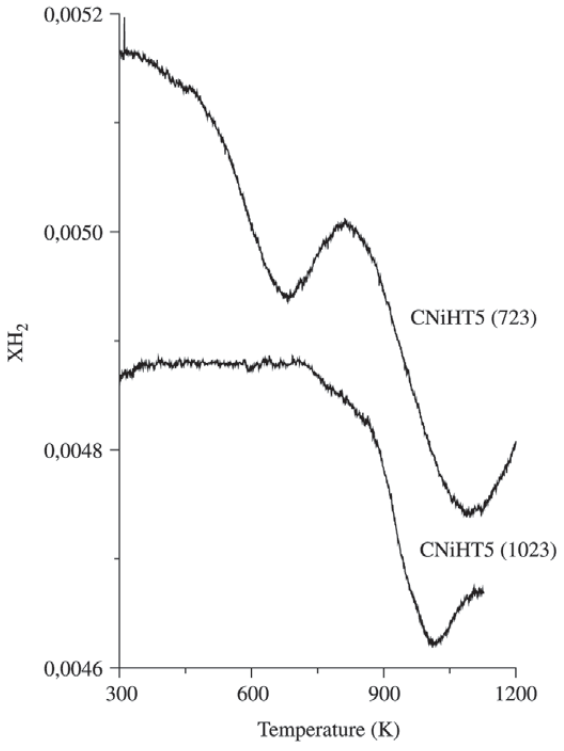

Figure 6. Thermoprogrammed reduction profile for NiHT5 calcined at 723 and 1023 K (TPR in the range of 298 to 1123 K, without the isothermic step at 1123 K for 2 h).

were detected indicating that both nickel and aluminum oxides species are well dispersed in the MgO matrix.

Calcination up to 723 or 1023 K formed Ni,Mg,Al-mixed oxides with specific surface areas and pore volumes higher than those for the parent HTLC. The textural characteristics of both HTLCs and mixed oxides were also not influenced by differences in the nickel content.

Thermoprogrammed reduction analysis showed the presence of different Ni-containing oxide species on the calcined samples. H_2 consumption profiles were influenced both by Ni content and calcination temperature, indicating that these parameters influenced the nature and the strength of the interactions between Ni species and Mg(Al)O phase. Although the reduction of nickel has not complete for all samples, Ni^0 showed good dispersion (65 to 80%), which can be an important property for the future use of these materials as bifunctional catalysts with both hydrogenating and basic properties.

References

1. Cavani, F.; Trifiro, F.; Vaccari, A. *Catalysis Today*, v. 11, p. 173-301, 1991.
2. Reichle, W.T. *Chemtech*. v. 16, p. 58-63, 1986.
3. McKenzie, A.L.; Fishel, C.T.; Davis, R.J. *Journal of Catalysis*, v. 138, p. 547-561, 1992.
4. Tichit, D.; Lhouty, M.H.; Guida, A.; Chiche, B.H.; Figueras, F.; Auroux, A.; Bartalini, B.; Garrone, E. *Journal of Catalysis*, v. 151, p. 50-59; 1995.
5. Reichle, W.T.; Kang, S.Y.; Everhardt, D.S. *Journal of Catalysis*, v.101, p.352-359, 1986.
6. Corma, A.; Fornés, V.; Rey, F. *Journal of Catalysis*, v. 148, p. 205-212, 1994.
7. Del Arco, M.; Martin, C.; Martin, I.; Rives, V.; Trujillano R. *Spectrochimica Acta*, v. 49A, n. 11, p. 1575-1582, 1993.
8. Rey, F.; Fornés, V.; Rojo, J.M. *Journal of Chemical Society Faraday Transactions*, v. 88, n. 15, p. 2233-2238, 1992.
9. Di Cosimo, J.I.; Díez, V.K.; Xu, M.; Iglesia, E.; Apestegía, C.R. *Journal of Catalysis*, v. 178, p. 499-510, 1998.
10. Sharper, H.; Berg-Slot, J.J.; Stork, W.H.J. *Applied Catalysis*, v. 54, p. 79-87, 1989.
11. Velu, S.; Swamy C.S. *Applied Catalysis A: General*, v. 119, p. 241-252, 1994.
12. Climent, M.J.; Corma, A.; Iborra, S.; Primo, J. *Journal of Catalysis,* v. 151, p. 60-66, 1995.
13. Casenave, S.; Martinez, H.; Guimon, C.; Auroux, A.; Hulea, V.; Cordoneanu, A.; Dumitriu, *Thermochimica Acta*, v. 379, p. 85-931, 2001.
14. Corma, A.; Fornés, V.; Martin-Aranda, R.M. *Journal of Catalysis*, v. 134, p. 58-65, 1992.
15. Corma, A.; Martin-Aranda, R.M. *Applied Catalysis A: General*, v. 105, n. 2, p. 271-279, 1993.
16. Corma, A.; Iborra, S.; Primo, J.; Rey, F. *Applied Catalysis A: General*, v. 114, p. 215-225, 1994.
17. Cativela, C.; Figueras, F.; Fraille, J.M.; Garcia, J.J.; Mayoral, J.M. *Tetrahedron Letters*, v. 36,n. 23, p. 4125-4128, 1995.
18. Guida, A.; Lhouty, M.H.; Tichit, D.; Figueras, F.; Geneste, P. *Applied Catalysis A: General,* v. 164, p. 251-264, 1997.
19. Rao, K.K.; Gravelle, M.; Valente, J.S.; Figueras, F. *Journal of Catalysis*, v. 173, p. 115-121, 1998.
20. Noda, C.; Alt, G.P.; Werneck, R.M.; Henriques, C.A.; Monteiro, J.L.F. *Brazilian Journal of Chemical Engineering*, v. 15, n. 2, p. 120-125, 1998.
21. Roelofs, J.C.A.A.; van Dillen, J.A.; de Jong, P.K. *Catalysis. Letters*, v. 74, n. 1-2, p. 91-94, 2001.
22. Titulaer, M.K.; Ben, J.; Jansen, H.; Geus, J.W. *Clays Clay Minerals*, v. 42, p. 249-258, 1994.
23. Clause, O.; Rebours, B.; Merlen, E.; Triffiro, F.; Vaccari, A. *Journal of Catalysis*, v. 133, p. 231-246, 1992.
24. Clause, O.; Coelho, M.G.; Gazzano, M.; Matteuzzi, D.; Triffiro, F.; Vaccari, A. *Applied Clay Science*, v. 8, p. 169-179, 1993.
25. Quian, M.; Zeng, H.C. *Journal of Material Science*, v. 7, p. 493-504, 1997.
26. Kannan, S.; Velu, S.; Ramkumar, V.; Swamy, C.S. *Journal of Material Science*, v. 3, p. 1462-1474, 1995.
27. Basile, F.; Basini, L.; Fornasari, G.; Gazzano, M.; Triffiro, F.; Vaccari, A. *Chemical Communications*, p. 2435-2436, 1996.
28. Li, J.; Zhang, W.; Gao, L.; Gu, P.; Sha, K.; Wan, H. *Applied Catalysis A: General*, v. 165, p. 411-417, 1997.
29. Palomares, A.E.; Lópes-Nieto, J.M.; Lázaro, F.J.; Lópes, A.; Corma, A. *Applied Catalysis B: Environmental*, v. 20, n. 4, p. 257-266, 1999.
30. Corma, A.; Palomares, A.E.; Rey, F.; Marques, F. *Journal of Catalysis*, v. 170, n. 1, p. 140-149, 1997.
31. Basile, F.; Basini, L.; D'Amore, M.; Fornasari, G.; Guarinoni, A.; Matteuzzi, D.; Del Piero, G.; Triffiro, F.; Vaccari, A. *Journal of Catalysis*, v. 173, p. 247-256, 1998.
32. Medina, F.; Tichit, D.; Coq, B.; Vaccari, A.; Dung, N.T. *Journal of Catalysis*, v. 167, p. 142-152, 1997.
33. Lebedeva, O.; Tichit, D.; Coq, B. *Applied Catalysis A: General*, v. 183, p. 61-71, 1999.
34. Chen, Y.Z.; Hwang, C.M.; Liaw, C.W. *Applied Catalysis A: General*, v. 169, p. 207-214, 1998.
35. Rodrigues, A.C.C.; Henriques, C.A.; Monteiro, J.L.F. *Actas XVIII Simposio Iberoamericano de Catalisis*, Porlamar, Venezuela, setembro, p. 2009-2015, 2002.
36. Fornasari, G.; Gazzano, M.; Matteuzzi, D.; Triffirò, F.; Vaccari, A. *Applied Clay Science*, v. 10, p. 69-82, 1995.
37. Tichit, D.; Medina, F.; Coq, B.; Dutarte, R. *Applied Catalysis A: General*, v. 159, p. 241-258, 1997.
38. Holland, T.J.B.; Redfern, S.A.T. *Mineralog. Magazine*, v. 61, p. 65-77, 1997.
39. Figueiredo, J.L.; Órfão, J.J. *2º Curso Iberoamericano sobre caracterização de Catalisadores e Adsorventes*, Cardoso, D., Jordão, M.H.; Machado, F. (Eds), Editora UFSCar, São Carlos, SP, Brasil, p. 1, 2001.
40. Ichikuni, N.; Murata, D.; Shimazu, S.; Uematsu, T. *Catalysis Letters*, v. 69, p. 33-36, 2000